A simple model for 1/f spectra in heart rate variability

James P. Gleeson[a] and Aneta Stefanovska[b]

[a] Applied Mathematics, University College Cork, Cork, Ireland;
[b] Physics Department, Lancaster University, Lancaster, LA1 4YB, UK.

ABSTRACT

Heart rate variability (HRV) measures cycle-to-cycle correlations in the instantaneous oscillation period of the heart. In this paper it is shown that a simple model process, consisting of a sum of uncoupled sinusoidal oscillators with slightly different frequencies, has a HRV spectrum with a 1/f scaling over a range of frequencies. This implies that the appearance of $1/f$ HRV spectra in experiments should not be considered evidence of oscillator coupling or other more complex dynamics. The origin of the 1/f scaling in the model is examined analytically, and its dependence upon the sampling of low-amplitude fluctuations of the process is highlighted.

Keywords: 1/f spectrum, heart rate variability, oscillator jitter.

1. INTRODUCTION

The appearance of $1/f$ spectra in measured heart rate variability (HRV) time series is a source of much interest.[1,2] In this paper we examine the possibility of applying recent results on exactly solvable $1/f$ spectra to simple multi-oscillator models of the heart rate, and give a partial answer to the question posed in Ref. 1: "Are typical $1/f$ spectra in fact the spectra of noisy coupled oscillatory processes with time-varying frequencies spanning a wide frequency interval?" Specifically, we examine the oscillatory process created by the sum of many independent oscillators and show that the variability (defined like the HRV in e.g. Fig 5 of Ref. 2) indeed exhibits a range of $1/f$ scaling in its spectrum. Although our results are for processes with only one main spike in their Fourier spectra (unlike the five-spike heartbeat ECG signal, see Fig 6(a) of Ref. 2) we believe that the provable $1/f$ spectrum in this case may provide a useful benchmark for characterizing HRV spectra and for modelling of the cardiovascular system using phase oscillators.

The remainder of this paper is structured as follows. In section 2 we introduce our model for the near-periodic process, comprising of the sum of many independent sinusoidal oscillations. Preliminary numerical experiments are reported in section 3. In section 4 we derive an analytical result for the HRV spectrum, and finally examine the important role of amplitude fluctuations in section 5.

2. THE MODEL

We consider the possibility that a near-periodic signal $x(t)$ (like the heartbeat signal) could be generated by a sum of many independent sinusoidal oscillators:

$$x(t) = \sum_{n=1}^{N} \cos(\Omega t + \omega_n t + \phi_n). \tag{1}$$

Here Ω is the main oscillation frequency; each individual oscillator oscillates at its own frequency $\Omega + \omega_n$, which differs only slightly from the mean frequency Ω. In fact the individual frequency deviations ω_n of the N oscillators are here considered to be random numbers with a known distribution. For instance, the Gaussian distribution

$$P(\omega) = \frac{1}{\sqrt{2\pi\omega_0^2}} e^{-\frac{\omega^2}{2\omega_0^2}} \tag{2}$$

Send correspondence to JPG: E-mail: j.gleeson@ucc.ie, Telephone: +353 21 490 3410

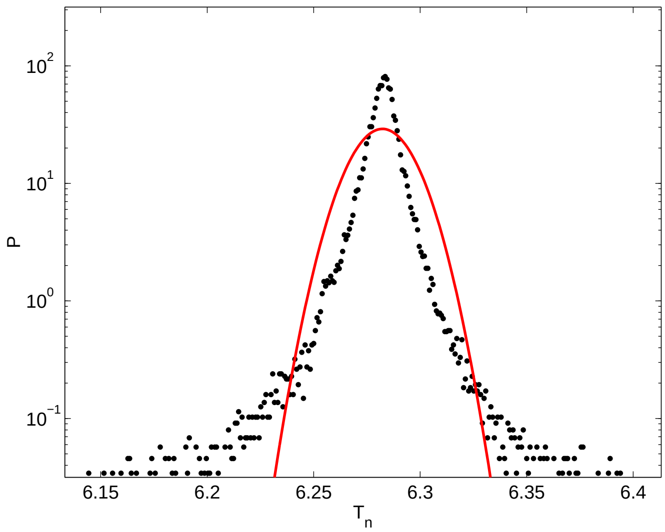

Figure 1. Histogram of T_n values, obtained from numerical calculation of zero-crossing intervals of the process (1). The solid line shows a Gaussian distribution with the same mean and variance as the data: note the data is markedly non-Gaussian, with a high peak and fat tails. Parameters are: $N = 100$, $\omega_0 = 10^{-3}$, $\Omega = 1$; statistics are obtained over 200 cycles in each of 500 realizations.

gives a convenient measure of the small deviation from the mean frequency by specifying that its standard deviation ω_0 obeys $\omega_0 \ll \Omega$. This scale-separation of the frequencies means that the frequency of any independent oscillator $(\Omega + \omega_n)$ is very close to Ω—we say the oscillators are 'near-identical'. The spectrum of the process $x(t)$ has a Gaussian lineshape (of standard deviation ω_0), centered at the main oscillation frequency Ω. The initial phases ϕ_n are uniformly-distributed random numbers on $[0, 2\pi]$.

Next we introduce some convenient notation. It is easy to show that the signal $x(t)$ may be written as

$$x(t) = f(t)\cos(\Omega t) + g(t)\sin(\Omega t), \tag{3}$$

where $f(t)$ and $g(t)$ are independent zero-mean Gaussian random functions with autocorrelation function

$$\frac{\langle f(t')f(t'+t)\rangle}{\langle f(t')^2\rangle} = \frac{\langle g(t')g(t'+t)\rangle}{\langle g(t')^2\rangle} = e^{-\frac{w_0^2 t^2}{2}}. \tag{4}$$

Throughout this paper we use angle brackets to denote averaging over an ensemble of realizations. Written in terms of an amplitude $r(t)$ and phase deviation $\theta(t)$, the signal $x(t)$ is

$$x(t) = r(t)\cos\left(\Omega t + \theta(t)\right), \tag{5}$$

with the time-varying amplitude and phase related to $f(t)$ and $g(t)$ by

$$\begin{aligned} r(t) &= \sqrt{f(t)^2 + g(t)^2} \\ \theta(t) &= -\tan^{-1}\frac{g(t)}{f(t)}. \end{aligned} \tag{6}$$

For the Gaussian processes $f(t)$ and $g(t)$ this form allows us to apply some known results. For instance, the amplitude $r(t)$ has probability density function

$$P(r) = \frac{2r}{N}\, e^{-\frac{r^2}{N}}, \tag{7}$$

and fluctuates on the timescale $1/\omega_0$, i.e. much more slowly than the oscillation timescale $1/\Omega$. The phase speed (time derivative of $\theta(t)$) is

$$v(t) = \frac{d}{dt}\theta(t), \tag{8}$$

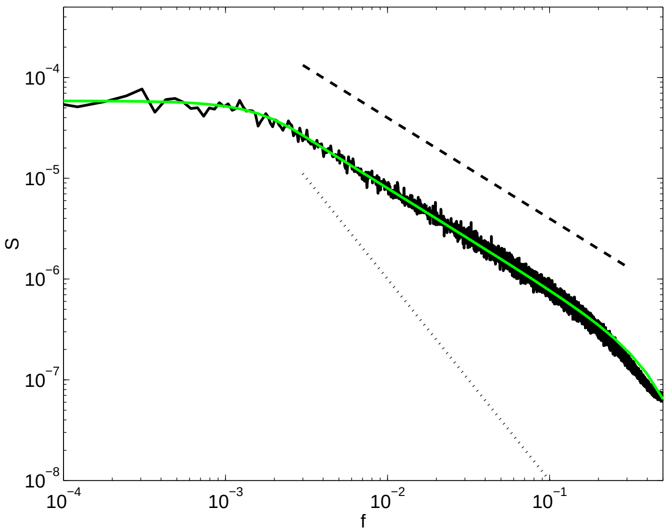

Figure 2. Numerical spectrum obtained from discrete Fourier transforms of H_n series (averaged over 100 realizations of 2^{14} samples). The green curve is the analytical prediction S_h from equation (22). Parameters are: $N = 100$, $\omega_0 = 10^{-3}$, $\Omega = 1$. The dashed line has slope -1, corresponding to a $1/f$ power-law scaling; for reference, the dotted line has slope -2, corresponding to a $1/f^2$ scaling.

and $v(t)$ is known (see Refs. 3–5) to be a stationary, zero-mean process with a spectrum scaling as $1/f$ for large frequencies $f \to \infty$. In this paper we investigate the connection between the spectra of the phase speed $v(t)$ and of the variability (HRV), the latter quantity having the advantage of being easily measured in experiments.

3. HRV AND ITS SPECTRUM

Our focus in this paper in on the statistics of the variability (e.g. HRV), which relate to the distance between zero up-crossings of $x(t)$. Denoting the zero up-crossing times by t_n $(n = 0, 1, 2, \ldots)$, the time between successive such crossings is

$$T_n = t_{n+1} - t_n, \tag{9}$$

and gives a measure of the instantaneous period of the oscillatory signal $x(t)$. Because the dominant frequency of the signal is Ω, the values of the time series T_n are distributed about the mean value of $2\pi/\Omega$.

Figure 1 shows a histogram of T_n values, obtained by generating samples of the process (1) with $N = 100$ oscillators, and using a numerical root-finding procedure to determine the zero-crossing times. Here we choose $\Omega = 1$ and $\omega_0 = 10^{-3}$; note the scale separation $\omega_0 \ll \Omega$ is respected. The distribution of T_n values is markedly non-Gaussian, with a high peak at the mean period $2\pi/\Omega$, and fatter-than-Gaussian tails for relatively large deviations from the mean.

To obtain information on the correlation between successive T_n values for a near-periodic signal, it is common practice to examine the time series of the variability (HRV) H_n defined (see Fig 5 of Ref. 2) as an interpolation of the discrete values

$$H_n = \frac{1}{T_n} \tag{10}$$

recorded at the times t_n. The spectrum of the HRV is easily obtained by Fast Fourier Transforming samples from the H_n time series generated in the numerical experiments. The resulting spectrum is shown in Figure 2. Note the $1/f$ scaling which is evident between a low-frequency limit of order ω_0 and a high-frequency limit of order Ω. The $1/f$ scaling spans the frequency range between these limits; in particular we note that as ω_0 is decreased (lowering the dispersion in oscillator frequencies), the lower limit of the $1/f$ scaling in the HRV spectrum is also decreased. In this way the $1/f$ scaling can be extended to arbitrarily low frequencies.

4. ANALYSIS OF THE MODEL

In this section we show how previous results[3, 5] on the phase speed process $v(t)$ can be used to understand the scaling of the HRV spectrum seen in Fig. 2.

Recall the instantaneous period of $x(t)$ in the nth oscillator cycle is given by $T_n = t_{n+1} - t_n$, with the zero up-crossing times t_n $(n = 0, 1, 2, \ldots)$ determined (from equation (5)) by the the implicit equation

$$\Omega\, t_n + \theta(t_n) = 2\pi n + \frac{3\pi}{2}. \tag{11}$$

Introducing the phase speed $v(t)$ defined in equation (8), we obtain the relation

$$\begin{aligned} T_n &= \frac{2\pi}{\Omega} - \frac{1}{\Omega}\left(\theta(t_{n+1}) - \theta(t_n)\right) \\ &= \frac{2\pi}{\Omega} - \frac{1}{\Omega}\int_{t_n}^{t_n+T_n} v(s)ds. \end{aligned} \tag{12}$$

An approximation valid when fluctuations are small, i.e. when the integral term is much smaller than $2\pi/\Omega$, is given by altering the upper integration limit to obtain an explicit formula for T_n in terms of an integral over the phase speed:

$$T_n \approx \frac{2\pi}{\Omega} - \frac{1}{\Omega}\int_{t_n}^{t_n+\frac{2\pi}{\Omega}} v(s)ds. \tag{13}$$

Under the same assumption, we can approximate H_n by the first term in its expansion for small v:

$$H_n = \frac{1}{T_n} \approx \frac{\Omega}{2\pi} + \frac{\Omega}{(2\pi)^2}\int_{t_n}^{t_n+\frac{2\pi}{\Omega}} v(s)ds + \ldots. \tag{14}$$

To examine the power spectrum we take the zero-mean quantity $H_n - \langle H_n\rangle$ and replace t_n by the continuous time variable t, i.e., we consider the spectrum of the continuous process

$$h(t) = \frac{\Omega}{(2\pi)^2}\int_{t}^{t+\frac{2\pi}{\Omega}} v(s)ds, \tag{15}$$

as an approximation to the (discrete) spectrum of the HRV $H_n - \langle H_n\rangle$. We first note that $h(t)$ has mean zero:

$$\langle h(t)\rangle = 0, \tag{16}$$

and that the spectrum of $v(t) = -d/dt\left(\tan^{-1} g/f\right)$ is known to have a $1/f$ high-frequency tail.[3] The Fourier transform $\hat{h}(f)$ is defined as usual by

$$\hat{h}(f) = \int_{-\infty}^{\infty} e^{-ift} h(t)dt, \tag{17}$$

with inverse transform

$$h(t) = \frac{1}{2\pi}\int_{-\infty}^{\infty} e^{ift}\hat{h}(f)df. \tag{18}$$

From equation (15) $h(t)$ may be expressed in terms of the Fourier transform $\hat{v}(f)$ of $v(t)$ as

$$\begin{aligned} h(t) &= \frac{\Omega}{(2\pi)^2}\int_{t}^{t+\frac{2\pi}{\Omega}} \frac{1}{2\pi}\int_{-\infty}^{\infty} e^{ifs}\hat{v}(f)df\ ds \\ &= \frac{\Omega}{(2\pi)^3}\int_{-\infty}^{\infty} \hat{v}(f)\frac{1}{if}e^{ift}\left(e^{2\pi i\frac{f}{\Omega}} - 1\right)df, \end{aligned} \tag{19}$$

and so (by comparison with (18)) the Fourier transform $\hat{h}(f)$ is given by

$$\hat{h}(f) = \frac{\Omega}{(2\pi)^2}\frac{1}{if}\left(e^{2\pi i\frac{f}{\Omega}} - 1\right)\hat{v}(f). \tag{20}$$

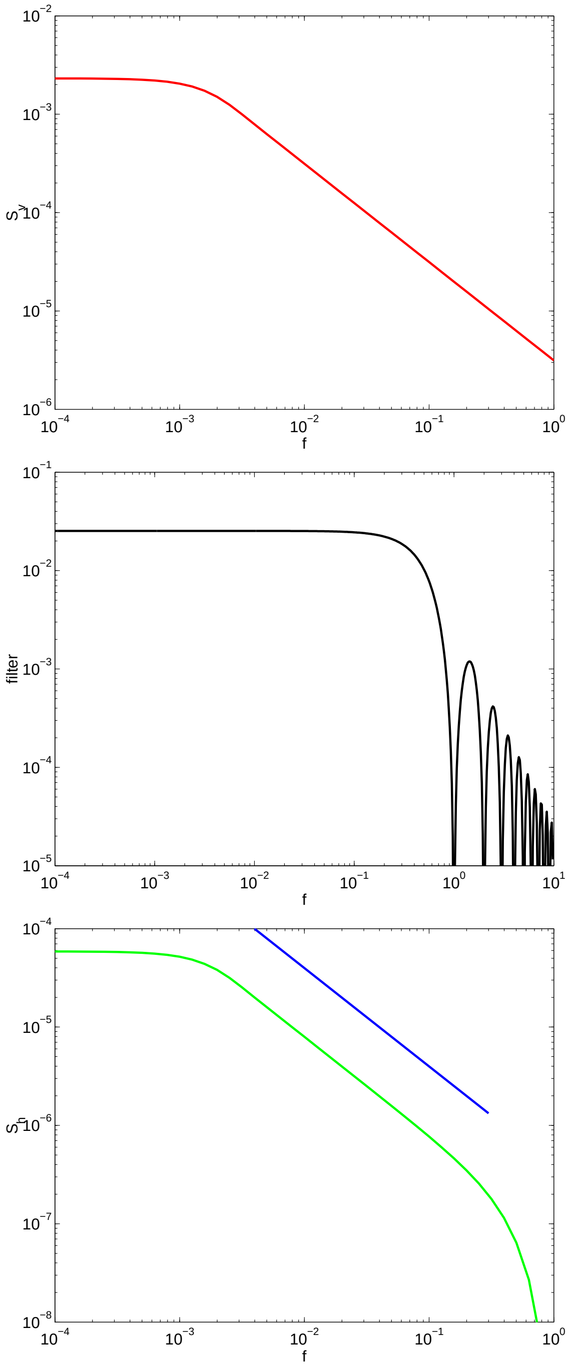

Figure 3. (a) The spectrum S_v of the stationary process $v(t) = -d/dt\,\tan^{-1}(g/f)$; (b) The filter function given by equation (25); (c) The product of S_v and the filter function, giving the spectrum S_h of the HRV-approximating $h(t)$. The blue line shows the $1/f$ behaviour of the spectrum. The parameter values here are $\omega_0 = 10^{-3}$ and $\Omega = 1$.

The power spectrum $S_h(f)$ of the process $h(t)$ is given by

$$S_h(f) = \frac{1}{\pi}\left\langle \hat{h}(f)\hat{h}^*(f)\right\rangle \tag{21}$$

with star denoting complex conjugate, and (20) relates this to the spectrum $S_v(f)$ of $v(t)$:

$$S_h(f) = \frac{\Omega^2}{(2\pi)^4}\frac{2}{f^2}\left[1-\cos\left(2\pi\frac{f}{\Omega}\right)\right]S_v(f). \tag{22}$$

According to equation (34) of Ref. 3 the spectrum of $v(t)$ is given by the integral

$$S_v(f) = -\omega_0^2\int_0^\infty \cos(ft)\ln\left(1-e^{-w_0^2t^2}\right)dt, \tag{23}$$

which has the large-f asymptotic form (see pp. 280-282 of Ref. 6)

$$S_v(f) \sim \pi\omega_0^2\frac{1}{f} \text{ as } f\to\infty. \tag{24}$$

The spectrum approaches a finite value as the frequency drops to zero — the low-frequency cutoff of the $1/f$ region is at $f\sim\omega_0$, see Fig. 3(a).

The spectrum of the HRV approximant is determined from (22) by multiplying $S_v(f)$ by the "filter function"

$$\frac{\Omega^2}{(2\pi)^4}\frac{2}{f^2}\left[1-\cos\left(2\pi\frac{f}{\Omega}\right)\right], \tag{25}$$

which is plotted in Fig. 3(b). Note that the filter is nearly constant for frequencies far below Ω. In the case under consideration, we have a separation of frequency scales from the low frequency ω_0 (characterizing the frequency of amplitude fluctuations) to the relatively fast oscillation frequency Ω, so that $\omega_0 \ll \Omega$. The combination (22) of the filter and the spectrum of v that gives the HRV spectrum is therefore expected to show a significant range of $1/f$ behaviour between the low-frequency cutoff ω_0 and the oscillation frequency Ω, i.e. we expect

$$S_h(f) \sim \begin{cases} \frac{1}{(2\pi)^2}S_v(0) & \text{for } f\ll\omega_0 \\ \frac{\omega_0^2}{4\pi}\frac{1}{f} & \text{for } \omega_0\ll f\ll\Omega, \end{cases} \tag{26}$$

with a more rapid decay of the power at frequencies higher than Ω, see Fig. 3(c).

5. INFLUENCE OF LOW-AMPLITUDE FLUCTUATIONS

In the preceding sections we have demonstrated (both numerically and analytically) a $1/f$ scaling in the HRV spectrum of the near-periodic process $x(t)$. With a view towards possible comparison with experiments, it is noteworthy that the amplitude $r(t)$ of the process $x(t)$ (defined in equation (5)) exhibits significant levels of variation, albeit over timescales of order $1/\omega_0$ (much longer than the mean oscillation period). In fact, it follows from equation (7) that the standard deviation of the amplitude is 52% of its mean value. In particular, the amplitude $r(t)$ occasionally reaches very low values, corresponding to maximal disorder among the individual oscillator phases. In this section we present numerical evidence demonstrating that these low-amplitude fluctuations are crucial for the the $1/f$ scaling observed in the HRV spectrum.

Figure 4 shows time series from a typical realization of $x(t)$ (with $N = 100$ oscillators, taking $\Omega = 1$ and $\omega_0 = 10^{-3}$ as before), over about 1000 oscillation periods. Figure 4(a) shows the amplitude $r(t)$, while the time series T_n is plotted in Fig. 4(b); both plots use the same timescale. Note that the two large deviations in the T_n series occur at times ($t_n \approx 500$ and $t_n \approx 4500$) when the amplitude $r(t)$ is at its lowest levels. This suggests that low-amplitude fluctuations in $x(t)$ may have strong effects on the T_n time series, and hence on the HRV spectrum.

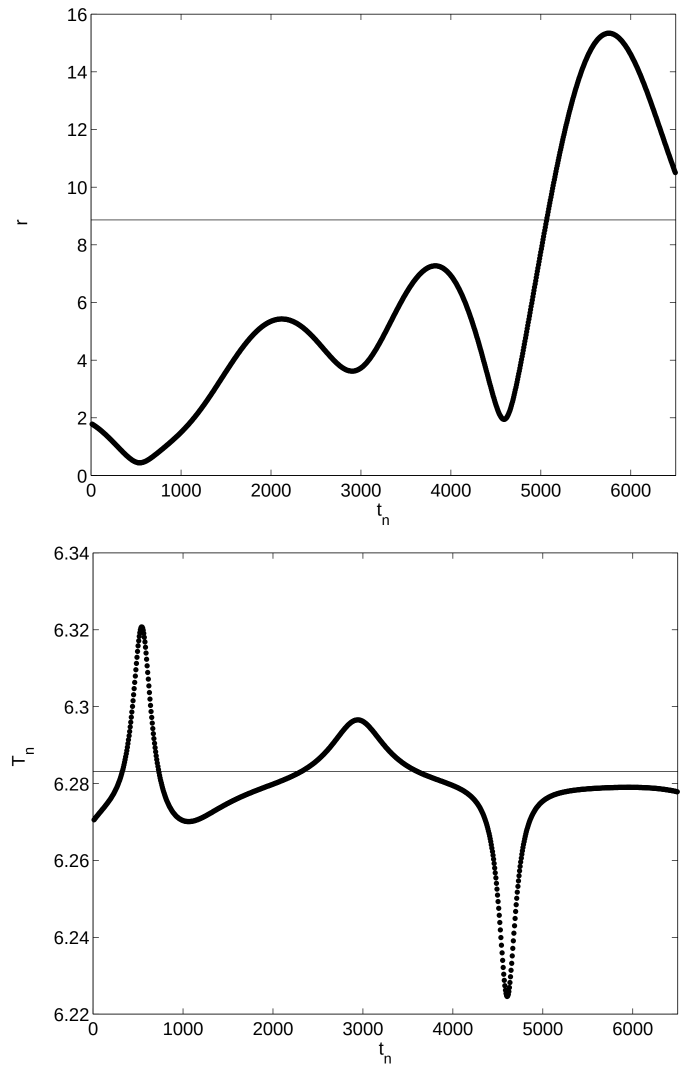

Figure 4. (a) The amplitude $r(t)$ of a single realization of $x(t)$, for parameters $\omega_0 = 10^{-3}$, $\Omega = 1$, and $N = 100$. (b) The time series T_n for the same realization as (a). The mean values of $r(t)$ and of T_n (over a large ensemble of samples) are indicated by the solid lines.

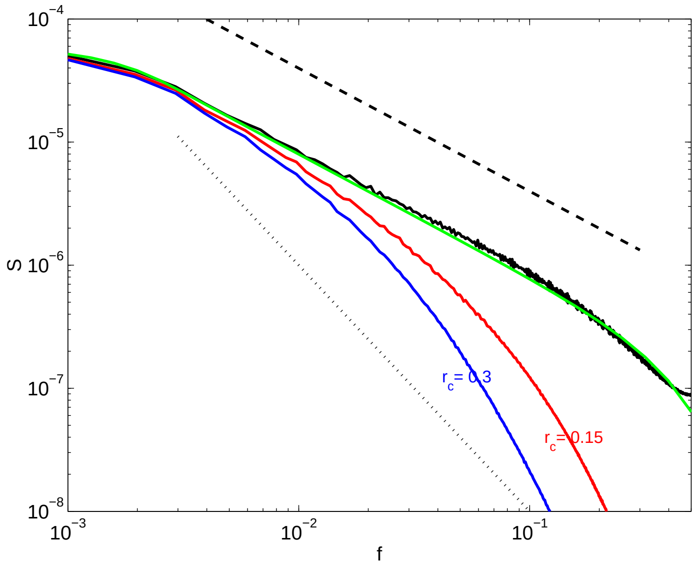

Figure 5. Numerical HRV spectrum (black line), using samples of 2^{10} oscillator cycles, averaged over 1000 realizations. The red line shows the spectrum found after rejecting any realizations in which the amplitude $r(t)$ falls below $r_c = 0.15$; the blue line is the corresponding spectrum with cutoff $r_c = 0.3$. For reference, the dashed line has slope -1 and the dotted line has slope -2; the analytical result (22) is shown in green.

To further investigate, we show in Figure 5 the HRV spectra obtained in three related numerical experiments. The black curve shows the spectrum found using 1000 realization of 2^{10} samples (sampled each oscillator period) of the H_n series: we find an excellent match to the theoretical result (22). For the other results shown, we choose a low-amplitude cutoff r_c and reject any realizations in which the amplitude $r(t)$ drops below r_c during the sampling window. The blue curve shows the spectrum corresponding to $r_c = 0.3$ (rejecting 15% of realizations), while the red curve is the spectrum for $r_c = 0.15$ (rejecting 9% of realizations). The $1/f$ scaling present in the $r_c = 0$ (black curve) case is clearly absent in the spectra where r_c is positive, leading to the conclusion that low-amplitude fluctuations of the process $x(t)$ are crucial to the generation of the $1/f$ spectrum in its HRV.

6. DISCUSSION

We have investigated a simple model (1) of a stochastic process $x(t)$ which is oscillatory on short timescales (or, in other words, which has a sharp peak at frequency Ω in its Fourier spectrum, with a narrow linewidth of order ω_0, and $\omega_0 \ll \Omega$). The HRV-like statistic for such a process has, under reasonable approximations, been shown to exhibit a $1/f$ range in its spectrum, specifically within the frequency range from ω_0 to Ω, see Fig. 2.

This model goes some way towards answering the question from Ref. 1 quoted in the Introduction. Especially noteworthy is the fact that our model uses only independent *uncoupled* oscillators to generate the signal $x(t)$, with the small variation in native oscillator frequencies causing a $1/f$ HRV spectrum. This implies that the appearance of $1/f$ HRV spectra should not be considered evidence of oscillator coupling or other more complex dynamics, and in this context our result is probably most useful as a 'null hypothesis'. We note however that the $1/f$ spectrum of $v(t)$ upon which our current results are based is also known to survive when the N oscillators are weakly coupled,[5] so that the $1/f$ HRV spectrum can also occur in this case.

Finally, we have shown that the $1/f$ scaling of the HRV spectrum depends sensitively upon sampling of low-amplitude fluctuations of the process $x(t)$—these fluctuations correspond to maximum disorder among the phases of the individual oscillators. Strong coupling of the oscillators make low-amplitude fluctuations of the mean field increasingly rare, and eliminates the mechanism for $1/f$ spectra discussed here.[5]

ACKNOWLEDGMENTS

The work of JPG is supported by Science Foundation Ireland under Investigator Award 02/IN.1/IM062.

REFERENCES

1. A. Stefanovska and I. Khovanov *Proc. Unsolved Problem of Noise*, 2005.
2. A. Stefanovska and M. Bračič *Cont. Phys.* **40**, pp. 31–55, 1999.
3. J. P. Gleeson *Phys. Rev. E* **72**, p. 011106, 2005.
4. B. R. Levin, *Theoretical basis of statistical radio engineering (Teoreticheskie osnovy statisticheskoi radiotekhniki)*, (in Russian) Sovetskoe Radio, Moscow, 1966.
5. J. P. Gleeson *EuroPhys. Lett.* **73**, pp. 328–344, 2006.
6. C. M. Bender and S. A. Orszag, *Advanced mathematical methods for scientists and engineers*, Springer, New York, 1999.